Journal of Environmental Chemical Engineering 14 (2026) 121537

Contents lists available at ScienceDirect

Journal of Environmental Chemical Engineering

journal homepage: www.elsevier.com/locate/jece

Photochemical degradation of the aromatic amine 4-(N,N-dimethylamino)benzonitrile: Triplet sensitisation, back reduction, and (quasi-)global modelling

Enmanuel Cruz Muñoz [a], Davide Ballabio [a], Viviana Consonni [a], Roberto Todeschini [a], Luca Carena [b], Iván Sciscenko [b], Silvio Canonica [c], Marco Minella [b], Davide Vione [b,*]

[a] Department of Earth and Environmental Sciences, University of Milano-Bicocca, P.zza della Scienza, 1, 20126 Milano, Italy
[b] Dipartimento di Chimica, Università di Torino, Via Pietro Giuria 5, Torino 10125, Italy
[c] Eawag, Swiss Federal Institute of Aquatic Science and Technology, Überlandstrasse 133, Dübendorf CH-8600, Switzerland

ARTICLE INFO

Keywords:
Fate of pollutants
Contaminants of emerging concern
Aromatic amines
Chromophoric dissolved organic matter
Surface-water photochemistry
Self-depuration of natural waters

ABSTRACT

Dissolved organic matter (DOM) acts as an inducer as well as an inhibitor in the photodegradation of 4-(N,N-dimethylamino)benzonitrile (DMABN), which undergoes both photodegradation by the excited triplet states of chromophoric DOM (^{3}CDOM*), and inhibition upon back reduction by the antioxidant moieties of DOM itself. On average, water with dissolved organic carbon (DOC) > 2.3 mgC L^{-1} would inhibit DMABN photodegradation by over 50 %. From the available data of [^{3}CDOM*] steady-state concentrations and the levels of DOC in lake water on a quasi-global scale (60°S-60°N latitude range), we were able to numerically assess the photochemical lifetimes of DMABN, here reported as year averages. Lifetimes of DMABN in lake water would amount to a couple of months or longer, and they would be the shortest in the tropical belt. Results of numerical calculations were interpolated using a suitable model function, with which an analytical equation was derived that relates DMABN lifetimes with lake depth, DOC, and latitude. For the first time to our knowledge, a general equation is here proposed to assess the photodegradation kinetics of a pollutant on a (quasi–)global scale.

1. Introduction

Trace organic contaminants (TrOCs) occur at low levels in natural waters, but they can substantially affect aquatic life forms through toxicity, endocrine disruption, and reproductive disorders. TrOCs can also pose a threat to human health through the use of water for irrigation, recreational activities, or as source of drinking water. Urban and agricultural runoff, industrial discharges, and urban wastewater, either treated or not, are major sources of TrOCs to aquatic environments [1]. Many of the relevant compounds are biorecalcitrant and polar, which help them by-pass traditional wastewater treatments such as biological degradation and adsorption [2]. The same features make it difficult for many TrOCs to undergo biodegradation in aquatic environments [3], where photodegradation is often a competitive reaction pathway.

Photodegradation in natural surface waters involves direct photolysis and indirect photochemistry [4]. Direct photolysis is triggered by the absorption of sunlight by the contaminant itself and proceeds through bond breaking, ionisation, or excited-state reactivity. In the case of indirect photochemistry, sunlight is absorbed by natural photoactive compounds (photosensitisers) such as nitrate, nitrite, and chromophoric dissolved organic matter (CDOM) [5,6]. Sunlight-excited photosensitisers produce a range of reactive transient species (photochemically produced reactive intermediates, PPRIs) that include the hydroxyl (·OH) and carbonate ($CO_3^{\bullet-}$) radicals, singlet oxygen ($^1O_2$), as well as CDOM triplet states (^{3}CDOM*) [7,8]. These PPRIs are involved in the photodegradation of contaminants [9,10]. In particular, reactions induced by ^{3}CDOM* are important in waters with high DOC (dissolved organic carbon) and cause the transformation of easily oxidised compounds such as, among others, phenols, anilines, sulfonamide antibiotics, thiols, and mercaptans. Very interestingly, the same compounds also tend to react fast with $CO_3^{\bullet-}$, which could induce degradation in the opposite (low DOC) conditions [11,12].

Natural organic matter typically favours the triplet-sensitisation processes that are responsible for contaminant degradation by ^{3}CDOM*, and which occur through transfer of electrons, hydrogen atoms, or energy. However, organic matter can also inhibit triplet

* Corresponding author.
E-mail address: davide.vione@unito.it (D. Vione).

https://doi.org/10.1016/j.jece.2026.121537
Received 2 December 2025; Received in revised form 14 January 2026; Accepted 29 January 2026
Available online 5 February 2026

sensitisation in the so-called back-reduction processes. Back reduction involves antioxidant, typically phenolic, moieties that reduce the contaminants partially oxidised (by ^{3}CDOM*) back to their parent compounds. The process is depicted in **reactions (1−3)**, where C is the contaminant and anti-oxidant DOM (AODOM) is a generic antioxidant moiety occurring in the dissolved organic matter [13–15].

$$^3\text{CDOM}^* + \text{C} \rightarrow \text{CDOM}^{\bullet-} + \text{C}^{\bullet+} \text{ [or (CDOM+H)}^\bullet + \text{(C-H)}^\bullet\text{]} \quad (1)$$

$$\text{C}^{\bullet+} \text{ [or (C-H)}^\bullet\text{]} \rightarrow \text{Products} \quad (2)$$

$$\text{C}^{\bullet+} \text{ [or (C-H)}^\bullet\text{]} + \text{AODOM} \rightarrow \text{C} + \text{AODOM}^{\bullet+} \text{ [or (AODOM-H)}^\bullet\text{]} \quad (3)$$

Triplet sensitisation and back reduction both play important roles in the environmental fate of aromatic amines. These toxic and potentially carcinogenic compounds are known to occur in natural surface waters at concentration levels that typically range from ng L^{-1} to μg L^{-1} [16]. The triplet sensitisation kinetics are known in detail for a few aromatic amines, among which there is the 4-(N,N-dimethylamino)benzonitrile (DMABN). The second-order reaction rate constants between DMABN and several triplet sensitisers are around 10^9 M^{-1} s^{-1} [17,18], and the knowledge of the rate constants facilitates the study of back-reduction phenomena in the presence of natural organic matter [13–18]. This issue makes DMABN a suitable model aniline to study the effects of the interplay between triplet sensitisation and back reduction. Furthermore, DMABN is used in the synthesis of benzoguanamine, which is a precursor of melamine resins used in the manufacture of dishes and kitchen furniture [19]. In this framework, the present work has the goal of studying DMABN back-reduction kinetics in natural waters samples, correlate it with the AODOM occurring in the same water samples (measured as the electron donating capacity, EDC), and assess the potential significance of triplet sensitisation/back reduction on a wide geographic scale. Actually, the kinetics of triplet sensitisation depend on the steady-state [^{3}CDOM*], while back-reduction is largely a function of the DOC. Recently, it has been possible to assess both quantities in global lake waters, included in the latitude belt between 60°S and 60°N [20]. The availability of this information enables the prediction of the photodegradation kinetics of contaminants that are degraded by ^{3}CDOM*, while also undergoing back reduction. In the case of DMABN, we also develop an equation that predicts photodegradation as a function of DOC, water depth, and latitude, which are currently available for lake waters worldwide.

2. Experimental section

2.1. Reagents and materials

The used chemical reagents were of analytical grade, and eluents for liquid chromatography were of gradient-grade purity. Further details are provided in the Supplementary Material (SM), ***Text SM1***.

Grab surface-water sampling was carried out in the Piedmont region (NW Italy) with 1 L Pyrex glass bottles, from the shores of four lakes (Avigliana, Maggiore, Candia and Viverone) and two paddy fields (Santhià and San Germano Vercellese). Water sampling took place in the month of January, 2017 (Jan 23rd for lakes and Jan 25th for paddies). The water samples were kept refrigerated during transport, vacuum filtered (cellulose acetate membranes, Sartorius, 47 mm diameter, 0.45 μm pore size), and stored under refrigeration for a maximum of ten days before use or analysis. This method of storage has been shown to be appropriate for the measurement of the photochemical reactivity of CDOM [21].

2.2. Irradiation experiments

The irradiation solutions (20 mL total volume) containing either DMABN or 2,4,6-trimethylphenol (TMP), the latter used as ^{3}CDOM* probe [11], were placed in quartz tubes (internal diameter 15 mm, external diameter 18 mm), which were tightly closed with glass stoppers. The tubes were irradiated in a DEMA (Hans Mangels GmbH, Bornhein-Roisdorf, Germany) model 125 merry-go-round photoreactor with nine positions, equipped with a Heraeus Noblelight TQ718 medium-pressure mercury lamp, operated at 500 W, and with a borosilicate glass cooling jacket. A 0.15 M $NaNO_3$ solution, passed through a Lauda RK 20 cooling thermostat, was used to keep the irradiated tubes at a temperature of 25.0 ± 0.5 °C, as well as to remove radiation < 320 nm so as to minimize the direct photolysis of DMABN. The photolysis of nitrate yields nitrite that absorbs till the visible region [22]. Therefore, the stability over time of the $NaNO_3$ solution was assessed by periodically checking that its transmittance at 360 nm (nitrite absorption maximum in the UV-A region) was above 85 % for the effective optical path length between the cooling jacket and the irradiation tubes (~3 cm). The photon flux in the quartz tubes was measured by chemical actinometry with 4-nitroanisole (5 μM) and pyridine (10 mM) [23], with variations below ±7 % during the irradiation experiments. The used lamp with filter solution emits several lines in the 320–600 nm wavelength range. A rough comparison of lamp emission in our set-up with mid-latitude sunlight irradiance is enabled by bacterial inactivation data [24], which suggest that the lamp intensity would be comparable to that of summertime sunlight. However, degradation kinetics observed under the lamp would still be considerably faster than in environmental lake waters (*vide infra*), due to very different optical pathways and water depths between the lamp set-up (cm-range) and the natural environment (several metres).

At scheduled irradiation times, 0.5 mL sample aliquots were withdrawn from each tube, placed in HPLC vials, and kept refrigerated till analysis that took place within 24 h from sampling.

2.3. Analytical determinations

The time trends of DMABN and TMP were monitored by high-performance liquid chromatography with diode-array detection (HPLC-DAD), using an Agilent 1100 chromatograph controlled with a Chromeleon 7 Chromatography Data System software. The instrument mounted a reverse-phase Cosmosil 5 C18-MS-II column (100 mm × 3 mm × 5 μm, 25°C). DMABN was eluted at 0.7 mL min^{-1} flow rate, with a 50 % A / 50 % B mixture of A = aqueous H_3PO_4 at pH 2.1 and B = acetonitrile, with retention time (t_R) of 3.3 min and detection at 298 nm. TMP was also eluted with 50 % A / 50 % B, with t_R = 3.0 min and detection at 210 nm.

The time trends of TMP and of DMABN were fitted with the exponential function $C_t = C_o\, e^{-k \cdot t}$, where C_t is the substrate (TMP or DMABN) concentration at the time t, C_o its initial concentration, and k the pseudo-first order degradation rate constant. The initial transformation rate was calculated as $R_o = k \cdot C_o$.

The natural water samples were characterised for the dissolved organic and inorganic carbon (DOC and DIC, respectively), using catalytic wet oxidation (DOC) and acidification / gas stripping (DIC), plus non-dispersive IR detection. We used a Shimadzu TOC-VCSH analyser, equipped with an ASI-V autosampler. The results of these determinations are reported in ***Table SM1***. The pH of the studied solutions was measured with a Thermo Scientific Orion® model 8115SC Ross™ combination semimicro pH electrode, connected to a Metrohm model 632 pH meter.

The EDC of the organic matter dissolved in the natural water samples was determined by size exclusion chromatography, combined with post-column reaction with the stable radical anion of 2,2'-azino-bis(3-ethylbenzothiazoline-6-sulfonate), $ABTS^{\bullet-}$ [25]. Water samples (2.5 mL) were injected into a Dionex Ultimate 3000 HPLC system (ThermoScientific, Sunnyvale, CA, USA) equipped with quaternary pump, autosampler, thermostated column compartment, photodiode array detector (PAD), and variable wavelength detector (VWD). We used a Toyopearl HW-50S column (8 × 300 mm, 30 μm; BGB, Boeckten, Switzerland), eluting with 50 mM borate buffer at a flow rate of

0.2 mL min^{-1}. After the PAD, set at 254 nm, the outflow was mixed with an $ABTS^{\bullet-}$ solution that was delivered at a flow rate of 0.04 mL min^{-1} with a Dionex PC 10 system, through a 750 μL knitted reaction coil (Dionex). Finally, the liquid flux reached the VWD, set at 405 nm (negative absorbance peak integration, [25]).

2.4. Photoreactivity maps

The assessment of DMABN photochemical reactivity by triplet sensitisation was carried out in the latitude band included between 60°S and 60°N, under yearly-averaged fair-weather sunlight. The depth and DOC values were taken from the worldwide lake databases of HydroLAKES ([26,27] and http://www.hydrosheds.org) and of Toming et al. [28,29]. The values of [^{3}CDOM*] in lake water between 60°S and 60°N latitude were taken from Carena et al. [30]. The ^{3}CDOM* calculations excluded lakes with depth $d < 5$ m, the water of which can easily become turbid upon stirring by the wind. Moreover, lakes located above 500 m a.s.l. were excluded because of the high probability of ice cover during winter, which prevents photochemical reactions from taking place. For the remaining $> 7 \times 10^4$ lakes, the steady-state [^{3}CDOM*] was calculated by considering incident sunlight irradiance, radiation absorption by the water column, as well as ^{3}CDOM* photogeneration and quenching [20]. The values of DOC and [^{3}CDOM*] were used to assess DMABN photodegradation kinetics by triplet sensitisation (*vide infra*). This approach has been shown to successfully predict photodegradation kinetics of clofibric acid in Lake Greifensee, Switzerland, which mainly proceed by triplet sensitisation [30,31].

Maps were generated with the QGIS software (version 3.2.3-Bonn) [32]. The dataset obtained for a given photochemical parameter y was divided into four colour-labelled groups, defined by considering the average (μ_y) and standard deviation (σ_y) of that dataset. In particular, the chosen intervals were: *(i)* $y < (\mu_y - \sigma_y)$; *(ii)* $(\mu_y - \sigma_y) < y < \mu_y$; *(iii)* $\mu_y < y < (\mu_y + \sigma_y)$, and *(iv)* $y > (\mu_y + \sigma_y)$.

2.5. Multivariate data analysis

Principal Component Analysis (PCA) was initially carried out to explore patterns in sample distributions and the correlations between longitude, latitude, DOC, depth, [^{3}CDOM*], and half-life time of DMABN, $t_{½,DMABN}$ [33]. PCA calculations were performed with the software CAT (Chemometric Agile Tool) as in a previous work [34].

Multivariate regression was subsequently carried out to establish a quantitative relationship between three independent variables (latitude, DOC, depth) and $t_{½,DMABN}$, which was considered as the dependent response. In order to consider non-linear relationships, some non-linear transformations were also considered as modelling variables. In particular, interactions between features and their squared and cubic effects were included. Regression was carried out by means of Ordinary Least Squares, and validation was performed by randomly splitting the dataset in training and test sets, with a 50 % proportion [35]. Training samples were used to calibrate the regression model, which was then used to predict the $t_{½,DMABN}$ values of the test samples, thereby assessing the predictive accuracy of the model itself. Regression models were calculated by means of the regression toolbox for MATLAB.

3. Results and discussion

3.1. DMABN photodegradation and back-reduction

The time trend of 5 μmol L^{-1} DMABN upon irradiation in lake and paddy-water samples is reported in Fig. 1a. DMABN was also irradiated in buffered ultra-pure water (5 mmol L^{-1} phosphate buffer) at pH 5.5 and 8.5, to get insight into its direct photolysis at different pH values. The reported time trends suggest that the direct photolysis process in the natural water samples would play a secondary role compared to indirect photochemistry. TMP was also irradiated under the same conditions, at

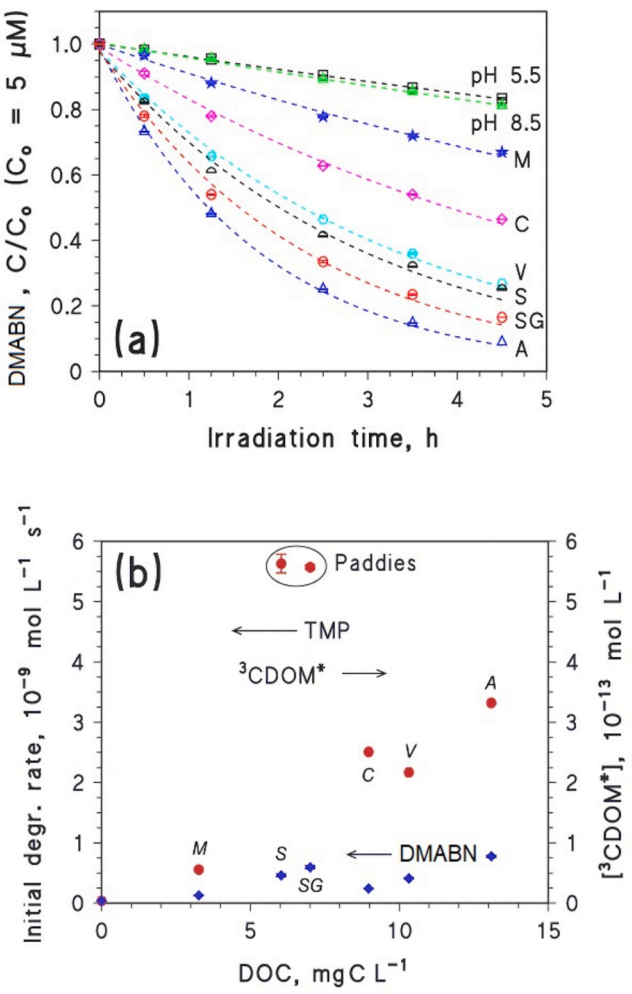

Fig. 1. **(a)** Time trends of 5 μmol L^{-1} DMABN, irradiated in buffered ultra-pure water (pH 5.5 and 8.5) and in different natural water samples (M: Lake Maggiore; C: Lake Candia; V: Lake Viverone; A: Lake Avigliana; S: Santhià; SG: San Germano Vercellese). S and SG are paddy fields. **(b)** Initial degradation rates of TMP (●) and DMABN (◆) (R_{TMP} and R_{DMABN}, respectively, left Y-axis), as a function of the DOC values of the irradiated water samples. The degradation rate of 5 μmol L^{-1} TMP was used to derive the steady-state [^{3}CDOM*], which is reported on the right Y-axis. The error bounds represent the standard error of replicate measurements.

5 μmol L^{-1} initial concentration. TMP undergoes negligible direct photolysis and it is commonly used as a ^{3}CDOM* probe [36], due to its selective reactivity towards triplet sensitisation and because [^{3}CDOM*] » [$^{\bullet}$OH] in irradiated natural waters. On the one side, given the reactivity difference between TMP and ^{3}CDOM* and between TMP and $^1O_2$, the contribution of $^1O_2$ to TMP photodegradation can be estimated to be < 6 %. On the other hand, the contribution by $^{\bullet}$OH to TMP photodegradation would be below 10 % because, although $^{\bullet}$OH and ^{3}CDOM* show similar reaction rate constants with TMP, [^{3}CDOM*] is at least an order of magnitude higher than [$^{\bullet}$OH] in most natural surface waters [36].

The initial degradation rates of TMP (R_{TMP}) and DMABN (R_{DMABN}) are reported in Fig. 1**b** (left Y-axis), as a function of the DOC values of the water samples. Note that each reported DOC value is referred to the given water sample before the spike with either TMP or DMABN, thus DOC = 0 mgC L^{-1} represents ultra-pure water. Both R_{TMP} and R_{DMABN} increased more or less linearly with increasing DOC in the case of lake water. In contrast, the rates in paddy water were considerably higher than the actual DOC values might suggest, especially for TMP (highlighted in the figure). Actually, previous research has shown that the

quantum yield of ^{3}CDOM* photogeneration ($\Phi_{^3CDOM^*}$) was about an order of magnitude higher in paddy water than in water taken from lakes located at mid latitude [37,38], which would be consistent with the R_{TMP} and [^{3}CDOM*] data reported in Fig. 1**b**. The most likely explanation for this difference is the higher contents of photoactive humic substances in paddy water as compared to typical lake water [38].

A reasonable assessment for the second-order reaction rate constant between TMP and ^{3}CDOM* is $k_{TMP,^3CDOM^*} \sim 2 \times 10^9$ L mol^{-1} s^{-1} [39], while the pseudo first-order deactivation rate constant of ^{3}CDOM* in aerated solution is $k_{^3CDOM^*} = 5 \times 10^5$ s^{-1} [40]. These rate constant values appear reasonable to describe the photochemical behaviour of lake water and paddy water [37,38,41]. In this framework, 5 μmol L^{-1} TMP would only scavenge 2 % of ^{3}CDOM*, with a negligible impact on the steady-state [^{3}CDOM*]. If we assume that the reported values of $k_{TMP,^3CDOM^*}$ and $k_{^3CDOM^*}$ are representative of the behaviour of the natural water samples investigated here, the initial degradation rate of TMP can be expressed as $R_{TMP} = k_{TMP,^3CDOM^*} \times [TMP]_o \times [^3CDOM^*]$, where [^{3}CDOM*] is practically independent of $[TMP]_o = 5$ μmol L^{-1}. This issue allows for the calculation of $[^3CDOM^*] = R_{TMP} (k_{TMP,^3CDOM^*} [TMP]_o)^{-1}$, the values of which, obtained from each relevant R_{TMP} datum, are also reported in Fig. 1**b** (right Y-axis).

Another interesting issue that can be seen in Fig. 1**b** is that $R_{TMP} > R_{DMABN}$. The second-order reaction rate constants of DMABN with several triplet sensitisers have been found to vary in the range of (0.03–5)× 10^9 L mol^{-1} s^{-1}, with most values > 2 × 10^9 L mol^{-1} s^{-1} [17]. This issue would imply $k_{DMABN,^3CDOM^*} \geq k_{TMP,^3CDOM^*}$, in contrast with our findings about reaction rates.

The inconsistency has two possible explanations: *(i)* $k_{DMABN,^3CDOM^*}$ is best represented by $k_{DMABN,^32AcN^*} = 2 \times 10^8$ L mol^{-1} s^{-1} (2AcN = 2-acetonaphthone) [17], so that $k_{DMABN,^3CDOM^*} < k_{TMP,^3CDOM^*}$ and/or, perhaps most likely, *(ii)* differently from TMP, DMABN undergoes back-reduction by the antioxidant moieties of DOM, which slows down its photodegradation.

Back reduction of DMABN$^{\bullet+}$ by both phenolic compounds and natural organic matter (Pony Lake Fulvic Acids, PLFA, and Suwannee River Fulvic Acids, SRFA) has been reported by Leresche et al. [17,18]. In the back-reduction scenario, in addition to the intrinsic reactivity of each substrate with ^{3}CDOM*, one expects a higher inhibition of DMABN photodegradation in high-DOC water as compared to TMP. The rationale is that, the higher the DOC is, the higher should also be the overall concentration of reducing moieties in the sample DOM [42]. In the case of DMABN, this issue would offset the fact that [^{3}CDOM*] would increase with increasing DOC [12].

In analogy with a previous study of sulfadiazine photodegradation [42], one might expect that the rate ratio $R_{TMP}\, R_{DMABN}^{-1}$ be proportional to the EDC of the water samples. Indeed, the EDC measures the concentration of anti-oxidant groups (AODOM) that could donate electrons to partially oxidised DMABN, giving back the initial compound in the process (**reactions 4,5**; [17,18]).

$$DMABN + {}^3CDOM^* \rightarrow DMABN^{\bullet+} + CDOM^{\bullet-} \quad (4)$$

$$DMABN^{\bullet+} + AODOM \rightarrow DMABN + AODOM^{\bullet+} \quad (5)$$

The plot of $R_{TMP}\, R_{DMABN}^{-1}$ *vs*. EDC is reported in Fig. 2**a**, which shows that the samples with the highest EDC values generally had the highest $R_{TMP}\, R_{DMABN}^{-1}$ ratios as well. The correlation between $R_{TMP}\, R_{DMABN}^{-1}$ and EDC is statistically significant ($p = 0.05$), despite the natural variability that would be caused by differences in CDOM and AODOM between different lake-water and paddy-water samples. Another cause for variability would be due to the involvement of additional PPRIs ($^{\bullet}$OH, $^1O_2$, $CO_3^{\bullet-}$) in the degradation of DMABN, but the observed correlation suggests that these additional processes would at most play a secondary role. It is also interesting to observe that the EDC values were the highest in the paddy water samples, where it was $R_{TMP} \gg R_{DMABN}$ (Fig. 1**b**).

Leresche et al. [18] have shown that the triplet-sensitised phototransformation of DMABN is inhibited by both PLFA and SRFA. They

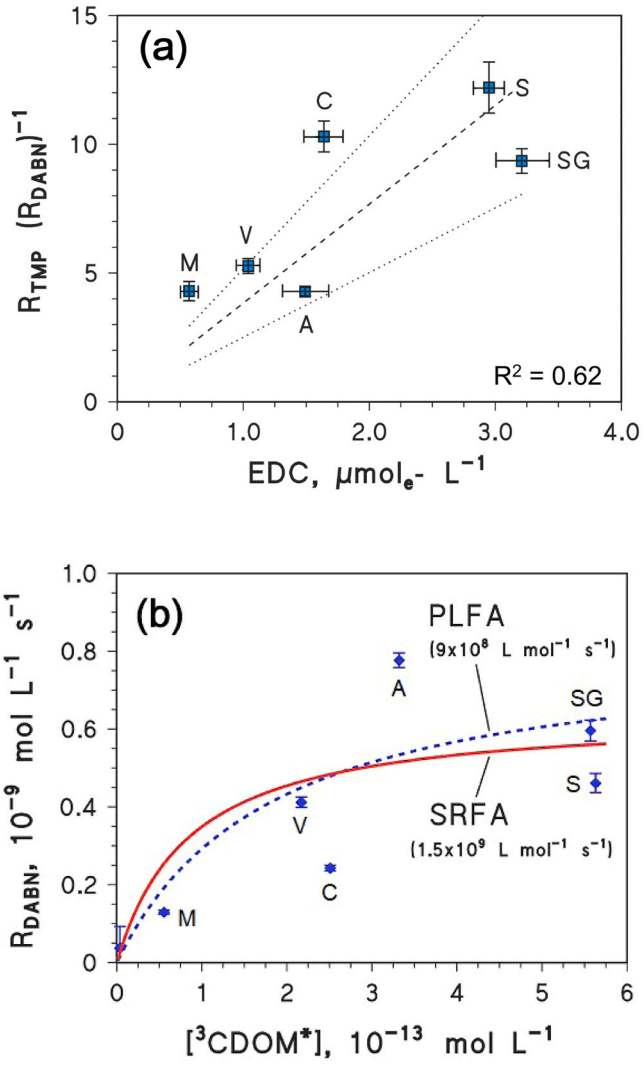

Fig. 2. **(a)** Ratio of R_{TMP} (R_{DMABN})$^{-1}$, as a function of the electron-donating capacity (EDC) of the irradiated water samples. **(b)** Plot of R_{DMABN} (the experimental data points are the same as (a)) as a function of [^{3}CDOM*], the latter derived from the R_{TMP} data obtained by irradiation of the same water samples. Model predictions are also reported for the PLFA-like and the SRFA-like scenarios (see the text for further details). The values within brackets are the fit estimates for the second-order reaction rate constants of TMP with ^{3}CDOM* ($k_{DMABN,^3CDOM^*}$).

have found that the initial degradation rate of DMABN, R_{DMABN}, can be conveniently expressed as follows:

$$R_{DMABN} = \frac{k_{DMABN,^3CDOM^*} \left[{}^3CDOM^*\right] [DMABN]_o}{1 + \frac{DOC}{[DOM]_{1/2}}} \quad (6)$$

where $[DMABN]_o = 5$ μmol L^{-1} and $[DOM]_{1/2}$ is the concentration of organic matter that halves the triplet-sensitised transformation of DMABN, compared to the case where no reducing moieties are present. In particular, it has been found that $[DOM]_{1/2} = 3.2$ mgC L^{-1} in the case of PLFA and $[DOM]_{1/2} = 1.5$ mgC L^{-1} in the case of SRFA [18].

Based on Eq. (6), one can calculate the expected values of R_{DMABN} as a function of [^{3}CDOM*], using the values of $[DOM]_{1/2}$ obtained in the PLFA-like and SRFA-like scenarios. The experimental data of R_{DMABN} *vs*. [^{3}CDOM*] are plotted in Fig. 2**b**. The figure also reports the prediction curves based on Eq. (6), for the PLFA-like and the SRFA-like scenarios [we used $[DOM]_{1/2} = 3.2$ mgC L^{-1} (PLFA-like scenario) and $[DOM]_{1/2} = 1.5$ mgC L^{-1} (SRFA-like scenario) as constants in the fit of the

experimental data with Eq. (6)].

The experimental data show variability, but the prediction curves fit them very reasonably and yield comparable values of the predicted second-order rate constants $k_{DMABN,^3CDOM^*}$. This result suggests the following issues: *(i)* Eq. (6) describes well the behaviour of DMABN in the presence of natural CDOM (as ^{3}CDOM* source) and AODOM, which supports the back-reduction scenario described by Leresche et al. [17,18] and suggests that the reactions of DMABN with additional PPRIs would be less important than triplet sensitisation; *(ii)* TMP behaved quite well as ^{3}CDOM* probe, which allowed for a consistent estimate of $k_{DMABN,^3CDOM^*}$; *(iii)* the values of $[DOM]_{1/2}$ obtained for PLFA and SRFA [17,18] are reasonably representative of the behaviour of natural organic matter in our samples as well, which allows for some generalisation of such values.

Because of the good agreement between the two estimates of $k_{DMABN,^3CDOM^*}$ in the PLFA-like and SRFA-like scenarios, it is reasonable to assume an average value $k_{DMABN,^3CDOM^*} = ½(k_{DMABN,^3CDOM^*(PLFA\text{-}like)} + k_{DMABN,^3CDOM^*(SRFA\text{-}like)}) = 1.2 \times 10^9$ L mol^{-1} s^{-1} as representative of natural waters. Such a value looks reasonable, because it is quite in the range of the reported second-order reaction rate constants between DMABN and the triplet states of model sensitisers [17]. Actually, our estimate of $k_{DMABN,^3CDOM^*}$ is in the lower range of these values, which makes sense when considering that the bulk of natural sensitisers typically shows lower reactivity when compared to most model compounds [11,43]. Similarly, it can be assumed that $[DOM]_{½} = ½\{[DOM(PLFA\text{-}like)]_{½} + [DOM(SRFA\text{-}like)]_{½}\} = 2.3$ mgC L^{-1}.

3.2. Global-scale assessment of DMABN triplet sensitisation / back reduction

From Eq. (6) it is possible to derive the pseudo-first-order rate constant of DMABN degradation, $k_{DMABN} = R_{DMABN}\,([DMABN]_o)^{-1}$, and the corresponding half-life time, $t_{½,DMABN} = \ln 2\,(k_{DMABN})^{-1}$. Therefore, $t_{½,DMABN}$ can be assessed as a function of [^{3}CDOM*] and DOC:

$$t_{1/2,DMABN} = \ln 2 \frac{1 + \frac{DOC}{[DOM]_{1/2}}}{k_{DMABN,^3CDOM^*}\left[^3CDOM^*\right]} \quad (7)$$

Using Eq. (7), it would be possible to carry out a quasi-global assessment of $t_{½,DMABN}$, exploiting the estimates of DOC and [^{3}CDOM*] that are available for the global lakes located between 60°S and 60°N latitude. Such an assessment has unavoidable limitations, which are mainly linked with the extent by which the known equation parameters can be extended to such a large geographic scale. The DOC estimates are probably the most reliable, because they have been validated against a number of available field data [28]. The calculated [^{3}CDOM*] values are based on the assumptions that the quantum yields of triplet-state production from irradiated CDOM are reasonably uniform and that the deactivation of ^{3}CDOM* has similar kinetics in different environments. These two hypotheses have reasonable founding, as far as available experimental data are concerned [37,40], but validation against field data is currently limited. Validation could for instance imply the successful prediction of the field photodegradation kinetics of contaminants that are mainly degraded by ^{3}CDOM* reactions, which finds two main obstacles: *(i)* there is a paucity of field photodegradation data, separated from other attenuation pathways (e.g., biodegradation, hydrolysis, phase transfer); *(ii)* selective reaction with ^{3}CDOM* alone only occurs for a few pollutants. In this framework, with our [^{3}CDOM*] database we have been able to predict the reported field photodegradation kinetics of clofibric acid in the epilimnion of Lake Greifensee [31] within a factor of 2 [30], which is a very good result but is also the only attempt at validation carried out to date. It is also interesting to point out that a similar model approach, based on known triplet sensitisation rate constants and estimated [^{3}CDOM*] values, has been able to predict quite well the photodegradation kinetics of atrazine in the Patuxent river estuary (MD, USA), which is expected to mainly proceed by ^{3}CDOM* reactions [44,45].

In the case of $k_{DMABN,^3CDOM^*}$, our estimate has been obtained upon irradiation of natural water samples and the value is also within the range of published reaction rate constants, but of course the actual values in lake waters could show considerable worldwide variations. Similar considerations hold for $[DOM]_{½}$.

That said, our estimate of DMABN photodegradation kinetics between 60°S and 60°N is reported in Fig. 3, which shows the quasi-global maps of [^{3}CDOM*] (**3a**), DOC (**3b**), and $t_{½,DMABN}$ (**3c**). Fig. 3**a** suggests that the values of [^{3}CDOM*] would be the highest at elevated Nordic latitudes (boreal hemisphere), despite the fact that the year-averaged, fair-weather sunlight irradiance is most intense in the tropical belt (see ***Figure SM1***) [20,46]. The most likely explanation for this finding is that the lakes located above 30°N latitude have, on average, higher DOC values compared to the lakes located elsewhere in the world [28] (see Fig. 3**b**). In the case of a substrate such as TMP, such an issue means that the photodegradation kinetics would be the fastest (and, therefore, the half-life times would be the shortest) at elevated Nordic latitudes. In contrast, Fig. 3**c** clearly shows that the lowest values of $t_{½,DMABN}$ (i.e., the fastest photodegradation of DMABN) would be found in the tropical belt (30°S-30°N) plus the eastern US (latitude around 30–45°N). The most likely explanation is back-reduction, which considerably slows down the triplet-sensitised degradation of DMABN in high-DOC waters.

According to our photochemical model, high-DOC lake waters would actually be detrimental to the photodegradation of DMABN (see ***Text SM2***), which is in apparent contradiction with the experimental results shown in Fig. 1**b**. However, it should be noted that the irradiation experiments were carried out with cm-range water depths, while the lake-water depths considered in the photochemical model were typically in the range of several meters to some tens meters. The steady-state [^{3}CDOM*] values would be given by the following equation [46]:

$$\left[^3CDOM^*\right] = \frac{\Phi_{^3CDOM^*}}{k_{^3CDOM^*}} \int_\lambda p^\circ(\lambda)\left[1 - 10^{-A_1(\lambda)\ d\ DOC}\right] d\lambda \quad (8)$$

where $\Phi_{^3CDOM^*} = 1.3 \times 10^{-3}$ is the quantum yield of ^{3}CDOM* photogeneration from irradiated CDOM, $k_{^3CDOM^*} = 5 \times 10^5$ s^{-1} is the pseudo first-order deactivation rate constant of ^{3}CDOM* in aerated solution (mostly upon reaction with dissolved O_2), $p^\circ(\lambda)$ is the incident spectral photon flux density of sunlight [Einstein L^{-1} s^{-1} nm^{-1}], $A_1(\lambda) = 45\ e^{-0.015\ \lambda}$ is the specific absorbance by CDOM [L mgC^{-1} m^{-1}], d is the water depth [m], and the dissolved organic carbon DOC has units of mgC L^{-1}.

Fig. 4 reports the calculated values of [^{3}CDOM*] for $d = 0.01$ and 10 m, which would be representative of our irradiation experiments and of many lake waters, respectively. It can be seen that, in both scenarios, the values of [^{3}CDOM*] would increase with increasing DOC. However, if the correction factor for back reduction ($\gamma = \{1 + DOC/[DOM]_{½}\}^{-1}$) is also taken into account and we assume $[^3CDOM^*_{corr}] = \gamma\ [^3CDOM^*]$, the corresponding plots of [^{3}CDOM*$_{corr}$] vs. DOC show interesting differences compared to those of [^{3}CDOM*]. In the case of $d = 1$ cm, [^{3}CDOM*$_{corr}$] would still increase with increasing DOC but, for $d = 10$ m, [^{3}CDOM*$_{corr}$] would in contrast decrease with DOC if DOC ≥ 2 mgC L^{-1}. When considering that it would be $R_{DMABN} = k_{DMABN,^3CDOM^*}\ [^3CDOM^*_{corr}]\ [DMABN]_o$, the data shown in Fig. 4 are consistent with both our experimental kinetics of DMABN photodegradation and our photochemistry calculations.

The rationale is that, for deep water columns, CDOM would soon saturate absorption: for $d = 10$ m and DOC = 1 mgC L^{-1}, CDOM would absorb over 93 % of the incoming radiation below 400 nm. At the same depth and for DOC = 2 mgC L^{-1}, radiation absorption by CDOM ($\lambda <$ 400 nm) would be over 99 %. A further increase in the DOC (and in CDOM as well) would thus hardly produce a significant increase in radiation absorption [47]. In these circumstances, the back-reduction effect can easily slow down photodegradation as the DOC increases.

In contrast, in very shallow (cm-range) water columns, the

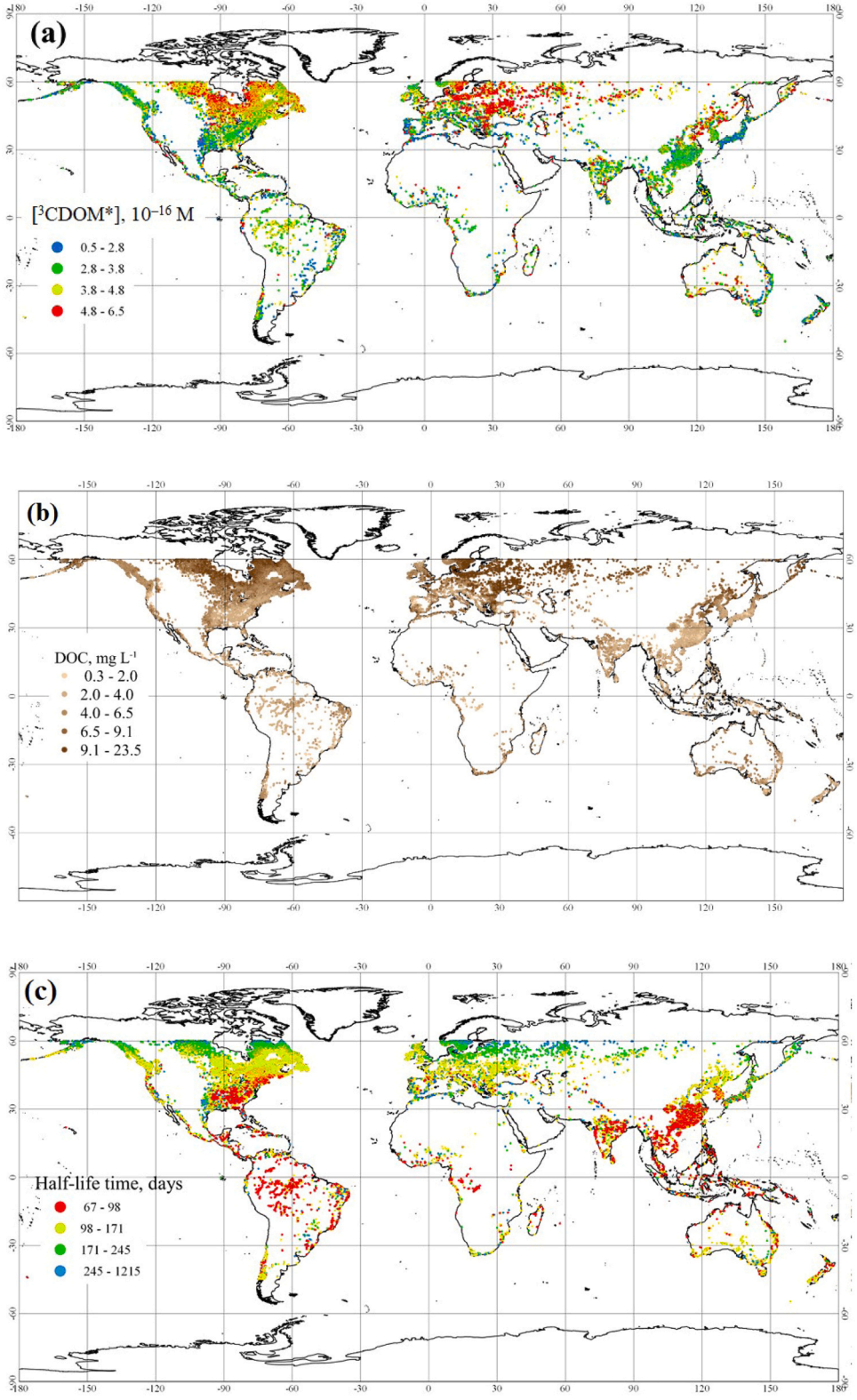

Fig. 3. **(a)** Quasi-global (60°S-60°N) map of the steady-state concentration of ^{3}CDOM* (multiplied by a factor of 10^{16}, thus $2.8 = 2.8 \times 10^{-16}$ M and so on). **(b)** Map of the DOC values in lake water. **(c)** Distribution of half-life time (days) of DMABN ($t_{½,DMABN}$) as assessed with Eq. (7). In all the maps, data are year-round averages.

absorption of radiation would not reach saturation that easily: for $d = 1$ cm and DOC = 1 mgC L^{-1}, CDOM would absorb over 0.25 % of the incoming radiation below 400 nm. For $d = 1$ cm and DOC = 2 mgC L^{-1}, absorption of the same radiation by CDOM would be over 0.50 %, an increase that is approximately proportional to the DOC increase. Moreover, the back-reduction effect at equal DOC would be the same at both $d = 1$ cm and $d = 10$ m (in both cases, $\gamma = 0.70$ for DOC = 1 mgC L^{-1}, and $\gamma = 0.53$ for DOC = 2 mgC L^{-1}). The combination of different degrees of absorption saturation with the same back-reduction effects explains why [^{3}CDOM*$_{corr}$] increases with increasing DOC at $d = 1$ cm,

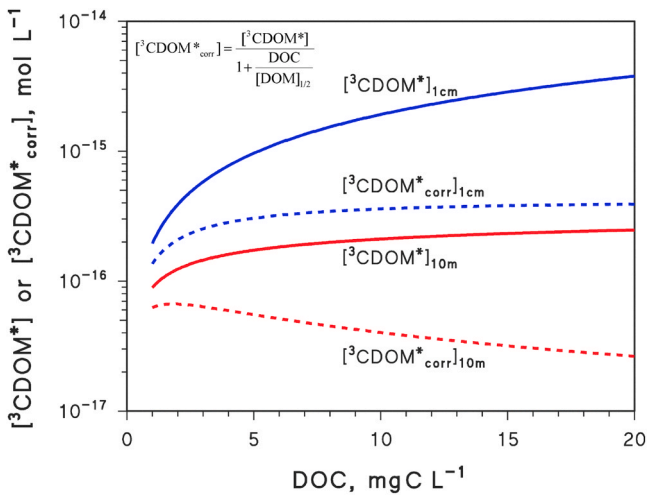

Fig. 4. DOC trends of the values of [^{3}CDOM*] (calculated according to Eq. (8)) and of [^{3}CDOM*$_{corr}$] = [^{3}CDOM*] (1 +DOC/[DOM]$_{½}$)$^{-1}$, for water depths of 1 cm (representative of irradiation experiments) and 10 m (representative of water columns in many lakes). Note that it would be $R_{DMABN} = k_{DMABN,^3CDOM^*}$ [^{3}CDOM*$_{corr}$] [DMABN]$_o$.

but has an opposite trend at $d = 10$ m.

As per Eq. (7), $t_{½,DMABN}$ would be a function of DOC and [^{3}CDOM*], since both $k_{DMABN,^3CDOM^*}$ and [DOM]$_{½}$ are constants. Moreover, in our approximation [20,30], [^{3}CDOM*] is a function of the DOC, the depth d, and the latitude Λ. Therefore, it should be possible to formulate an analytical equation that conveniently describes $t_{½,DMABN}$ vs. (DOC, d, Λ). This equation was actually found by non-linear data fitting ($R^2 > 99$ %; see ***Text SM2*** for calculation details), as follows:

$$t_{½,DMABN} = 22 + 8.8\,d - 1.4\,DOC - 0.11\,\Lambda + 0.89\,d\,DOC + 0.41\,DOC^2 - 0.16\,d^2 + 0.0016\,d^3 + 0.0001\,\Lambda^3 - 0.015\,DOC^3 \quad (9)$$

where the relevant measure units are: $t_{½,DMABN}$ [days]; DOC [mgC L^{-1}]; d [m]; Λ [degrees]. Since DOC and the depth d appeared to be the most important variables for modelling, we also explored contour plots of $t_{½,DMABN}$ as a function of the two variables at different levels of latitude (Fig. 5). It can be seen that d is detrimental to photodegradation, as expected. The DOC is also detrimental, although less than d, because the back-reduction processes prevail over triplet sensitisation if the water column is deep enough, as mentioned above. Latitude has only a rather small effect on $t_{½,DMABN}$, which is also different from the latitude trend of the irradiance (see ***Figure SM1***). The most likely reason is that many lakes located at elevated northern latitudes are also high in DOC (see Fig. 3**b**), thus Λ and DOC are not independent variables. As a consequence, the latitude effect would not be a pure irradiance effect, but rather a mixture of contributions by both irradiance and the DOC.

4. Conclusions

Dissolved organic matter acts as both sensitiser and quencher for the photodegradation of the studied cyanoaniline, DMABN. In fact, this contaminant undergoes both triplet-sensitised degradation by ^{3}CDOM* and back-reduction by the antioxidant moieties of dissolved organic matter (AODOM). The latter can be quantified as the electron-donating capacity of the water samples, which measures the potential of organic matter to reduce the partially oxidised DMABN radicals back to the parent compound.

The half-life time of DMABN can be expressed as a function of DOC and [^{3}CDOM*], which allows for an assessment of $t_{½,DMABN}$ to be carried out in lake water on a (quasi-) global scale (60°S-60°N latitude range). Results showed that DMABN photodegradation would be the fastest in the tropical belt, because the opposite effects of triplet sensitisation and back-reduction (both enhanced at high DOC) would partially cancel out, leaving the irradiance of sunlight as the main factor to govern photodegradation.

Finally, a statistical study returned an equation (Eq. (9)) that predicts the lifetime of DMABN as a function of latitude, DOC, and water depth. To our knowledge, this is the first time that such an equation is derived for a given pollutant on a (quasi-)global scale. Interestingly, a similar approach could be applied to other contaminants that, like DMABN, prevalently undergo photodegradation by reaction with ^{3}CDOM*.

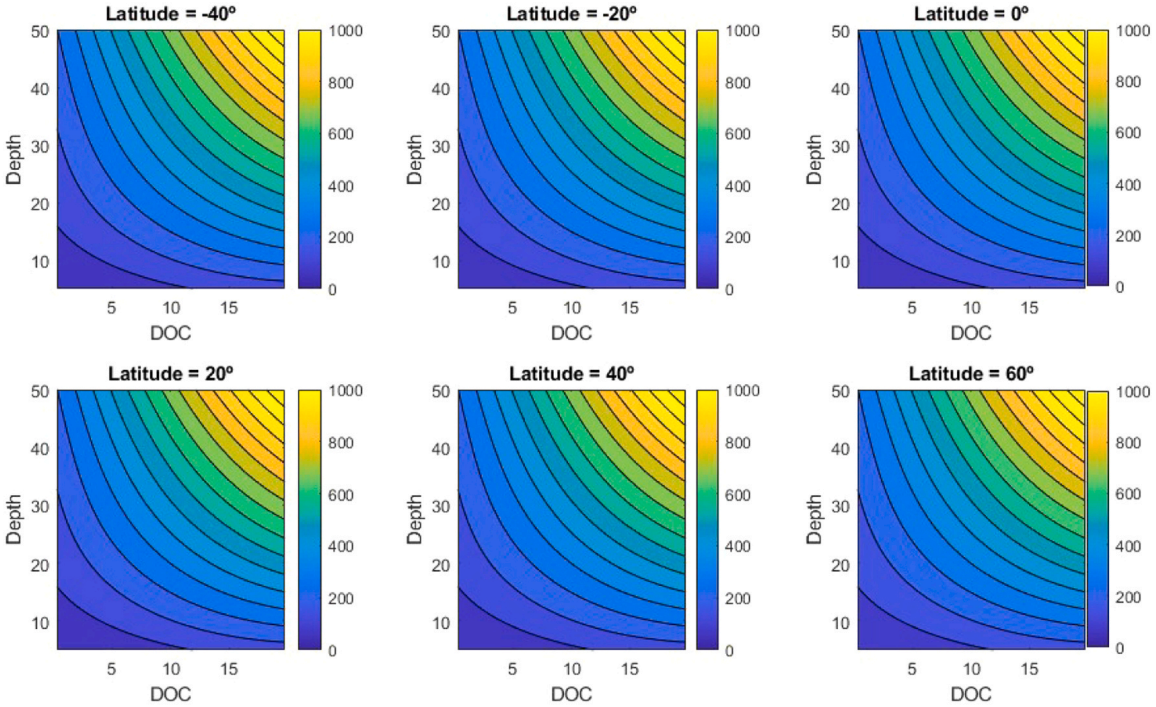

Fig. 5. Contour plots of $t_{½,DMABN}$ ([days], shown in different colours) as a function of the DOC ([mgC L^{-1}]) and depth ([m]), at different levels of latitude.

CRediT authorship contribution statement

Sciscenko Ivan: Writing – review & editing, Writing – original draft, Investigation, Funding acquisition, Data curation. **Silvio Canonica:** Writing – review & editing, Writing – original draft, Supervision, Conceptualization. **Luca Carena:** Writing – review & editing, Writing – original draft, Investigation, Data curation. **Enmanuel Cruz Muñoz:** Writing – review & editing, Writing – original draft, Investigation, Data curation. **Davide Ballabio:** Writing – review & editing, Validation, Supervision, Methodology. **Viviana Consonni:** Writing – review & editing, Validation, Data curation. **Roberto Todeschini:** Writing – review & editing, Software, Methodology. **Marco Minella:** Writing – review & editing, Validation, Supervision, Funding acquisition. **Davide Vione:** Writing – review & editing, Writing – original draft, Software, Funding acquisition, Conceptualization.

Declaration of Competing Interest

The authors declare that they have no known competing financial interests or personal relationships that could have appeared to influence the work reported in this paper.

Acknowledgements

We are grateful to Ursula Schönenberger and Elisabeth Muck (Eawag) for technical support. This study was funded by the European Union - NextGenerationEU, in the framework of the GRINS -Growing Resilient, INclusive and Sustainable project (GRINS PE00000018 – CUP D13C22002160001). The views and opinions expressed are solely those of the authors and do not necessarily reflect those of the European Union, nor can the European Union be held responsible for them. LC, MM and DV acknowledge support from the Project CH4.0 under the MUR program "Dipartimenti di Eccellenza 2023–2027" (CUP: D13C22003520001). IS acknowledges financial support by the Horizon Europe research and innovation programme Marie Sklodowska Curie Actions, PF grant agreement No. 101146398 (HERO4PFAS project).

Appendix A. Supporting information

Supplementary data associated with this article can be found in the online version at doi:10.1016/j.jece.2026.121537.

Data availability

Data will be made available on request.

References

[1] S.D. Richardson, T.A. Ternes, Water analysis: Emerging contaminants and current issues, Anal. Chem. 94 (2022) 382–416.
[2] F. Riva, E. Zuccato, C. Pacciani, A. Colombo, S. Castiglioni, A multi-residue analytical method for extraction and analysis of pharmaceuticals and other selected emerging contaminants in sewage sludge, Anal. Methods 13 (2021) 526–535.
[3] W.L. Desiante, N.S. Minas, K. Fenner, Micropollutant biotransformation and bioaccumulation in natural stream biofilms, Water Res 193 (2021) 116846.
[4] Z. Guo, D. Kodikara, L.S. Albi, Y. Hatano, G. Chen, C. Yoshimura, J. Wang, Photodegradation of organic micropollutants in aquatic environment: Importance, factors and processes, Water Res 231 (2023) 118236.
[5] Y. Xu, Y. Zhang, L. Qiu, M. Zhang, J. Yang, R. Ji, D. Vione, Z. Chen, C. Gu, Photochemical behavior of dissolved organic matter in environmental surface waters: A review, Eco Environ. Health 3 (2024) 529–542.
[6] Z. Luo, Y. Yan, R. Spinney, D.D. Dionysiou, F.A. Villamena, R. Xiao, D. Vione, Environmental implications of superoxide radicals: From natural processes to engineering applications, Water Res 261 (2024) 122023.
[7] H. Jiang, M. Zhao, W. Hong, W. Song, S. Yan, Mechanistic and kinetic consideration of the photochemically generated oxidative organic radicals in dissolved black carbon solutions under simulated solar irradiation, Environ. Sci. Technol. 58 (2024) 760–770.
[8] H. Sha, J. Nie, L. Lian, S. Yan, W. Song, Phototransformation of an emerging cyanotoxin (Aerucyclamide A) in simulated natural waters, Water Res 201 (2021) 117339.
[9] J.L. Packer, J.J. Werner, D.E. Latch, K. McNeill, W.A. Arnold, Photochemical fate of pharmaceuticals in the environment: Naproxen, diclofenac, clofibric acid, and ibuprofen, Aquat. Sci. 65 (2003) 342–351.
[10] R. Ossola, O.M. Jönsson, K. Moor, K. McNeill, Singlet oxygen quantum yields in environmental waters, Chem. Rev. 121 (2021) 4100–4146.
[11] K. McNeill, S. Canonica, Triplet state dissolved organic matter in aquatic photochemistry: reaction mechanisms, substrate scope, and photophysical properties, Environ. Sci. Process. Impacts 18 (2016) 1381–1399.
[12] D. Vione, A. Scozzaro, Photochemistry of surface fresh waters in the framework of climate change, Environ. Sci. Technol. 53 (2019) 7945–7963.
[13] S. Canonica, H.U. Laubscher, Inhibitory effect of dissolved organic matter on triplet-induced oxidation of aquatic contaminants, Photochem. Photobiol. Sci. 7 (2008) 547–551.
[14] J. Wenk, U. von Gunten, S. Canonica, Effect of dissolved organic matter on the transformation of contaminants induced by excited triplet states and the hydroxyl radical, Environ. Sci. Technol. 45 (2011) 1334–1340.
[15] J. Wenk, S. Canonica, Phenolic antioxidants inhibit the triplet-induced transformation of anilines and sulfonamide antibiotics in aqueous solution, Environ. Sci. Technol. 46 (2012) 5455–5462.
[16] Ö. Edebali, S. Krupčíková, A. Goellner, B. Vrana, M. Muz, L. Melymuk, Tracking aromatic amines from sources to surface waters, Environ. Sci. Technol. Lett. 11 (2024) 397–409.
[17] F. Leresche, L. Ludvíková, D. Heger, U. von Gunten, S. Canonica, Quenching of an aniline radical cation by dissolved organic matter and phenols: A laser flash photolysis study, Environ. Sci. Technol. 54 (2020) 15057–15065.
[18] F. Leresche, U. von Gunten, S. Canonica, Probing the photosensitizing and inhibitory effects of dissolved organic matter by using N,N-dimethyl-4-cyanoaniline (DMABN), Environ. Sci. Technol. 50 (2016) 10997–11007.
[19] X. Chen, S. Afreen, X. Yu, C. Dong, Q. Kong, Modified melamine-formaldehyde resins improve tensile strength along with antifouling and flame retardancy in impregnation of cellulose paper, RSC Adv. 9 (2019) 36788–36795.
[20] L. Carena, Á. García-Gil, J. Marugán, D. Vione, Global modeling of lake-water indirect photochemistry based on the equivalent monochromatic wavelength approximation: The case of the triplet states of chromophoric dissolved organic matter, Water Res 24 (2023) 120153.
[21] L. Carena, Y. Wang, S. Gligorovski, S. Berto, S. Mounier, D. Vione, Photoinduced production of substances with humic-like fluorescence, upon irradiation of water samples from alpine lakes, Chemosphere 319 (2023) 137972.
[22] J. Mack, J.R. Bolton, Photochemistry of nitrite and nitrate in aqueous solution: a review, J. Photochem. Photobiol. A Chem. 128 (1999) 1–13.
[23] D. Dulin, T. Mill, Development and evaluation of sunlight actinometers, Environ. Sci. Technol. 16 (1982) 815–820.
[24] M. Wegelin, S. Canonica, K. Mechsner, T. Fleischmann, F. Pesaro, A. Metzler, Solar water disinfection: Scope of the process and analysis of radiation experiments, J. Water Supply Res. Technol. Aqua 43 (1994) 154–169.
[25] K. Chon, E. Salhi, U. von Gunten, Combination of UV absorbance and electron donating capacity to assess degradation of micropollutants and formation of bromate during ozonation of wastewater effluents, Water Res 81 (2015) 388–397.
[26] M.L. Messager, B. Lehner, G. Grill, I. Nedeva, O. Schmitt, Estimating the volume and age of water stored in global lakes using a geo-statistical approach, Nat. Commun. 7 (2016) 13603.
[27] B. Lehner, M.L. Messager, HydroLAKES Tech. Doc. Version 1 (0) (2016).
[28] K. Toming, J. Kotta, E. Uuemaa, S. Sobek, T. Kutser, L.J. Tranvik, Predicting lake dissolved organic carbon at a global scale, Sci. Rep. 10 (2020) 8471.
[29] K. Toming, J. Kotta, E. Uuemaa, S. Sobek, T. Kutser, L.J. Tranvik, Predict. lake dissolved Org. Carbon a Glob. Scale [Data Set.] Zenodo (2020), https://doi.org/10.5281/zenodo.3452124.
[30] L. Carena, Á. García-Gil, J. Marugán, D. Vione, Global modeling of photochemical reactions in lake water: A comparison between triplet sensitization and direct photolysis, EcoEnviron. Heal 4 (2025) 100123.
[31] C. Tixier, H.P. Singer, S. Oellers, S.R. Müller, Occurrence and fate of carbamazepine, clofibric Acid, diclofenac, ibuprofen, ketoprofen, and naproxen in surface waters, Environ. Sci. Technol. 37 (2003) 1061–1068.
[32] QGIS Geographic Information System, Open Source Geospatial Foundation Project (2020).
[33] R. Bro, A.K. Smilde, Principal component analysis, Anal. Methods 6 (2014) 2812–2831.
[34] I. Sciscenko, A. Actis, E. Salvadori, A. Arques, C. Minero, F. Sordello, M. Minella, Ultraviolet-A light/oligomeric melem vs. visible light/graphitic carbon nitride towards H_2O_2 photoproduction and pollutants degradation: sometimes less is more, J. Environ. Chem. Engin 12 (2024) 114093.
[35] K. Varmuza, P. Filzmoser. Introduction to multivariate statistical analysis in chemometrics, 1st ed., CRC Press, Boca Raton, 2009.
[36] E. De Laurentiis, M. Minella, V. Maurino, C. Minero, M. Brigante, G. Mailhot, D. Vione, Photochemical production of organic matter triplet states in water samples from mountain lakes, located below or above the treeline, Chemosphere 88 (2012) 1208–1213.
[37] A. Marchisio, M. Minella, V. Maurino, C. Minero, D. Vione, Photogeneration of reactive transient species upon irradiation of natural water samples: Formation quantum yields in different spectral intervals, and implications for the photochemistry of surface waters, Water Res 73 (2015) 145–156.

[38] L. Carena, M. Minella, F. Barsotti, M. Brigante, M. Milan, A. Ferrero, S. Berto, C. Minero, D. Vione, Phototransformation of the herbicide propanil in paddy field water, Environ. Sci. Technol. 51 (2017) 2695–2704.
[39] F. Al Housari, D. Vione, S. Chiron, S. Barbati, Reactive photoinduced species in estuarine waters. Characterization of hydroxyl radical, singlet oxygen and dissolved organic matter triplet state in natural oxidation process, Photochem. Photobiol. Sci. 9 (2010) 78–86.
[40] S. Canonica, M. Freiburghaus, Electron-rich phenols for probing the photochemical reactivity of freshwaters, Environ. Sci. Technol. 35 (2001) 690–695.
[41] E. De Laurentiis, S. Buoso, V. Maurino, C. Minero, D. Vione, Optical and photochemical characterisation of chromophoric dissolved organic matter from lakes in Terra Nova Bay, Antartica. Evidence of considerable photoreactivity in an extreme environment, Environ. Sci. Technol. 47 (2013) 14089–14098.
[42] D. Vione, D. Fabbri, M. Minella, S. Canonica, Effects of the antioxidant moieties of dissolved organic matter on triplet-sensitized phototransformation processes: Implications for the photochemical modeling of sulfadiazine, Water Res 128 (2018) 38–48.
[43] L.De Brito Anton, A.I. Silverman, J.N. Apell, Comparing photodegradation model systems: measuring bimolecular rate constants between photochemically produced reactive intermediates and organic contaminants, Environ. Sci. Process Impacts 27 (2025) 2116–2127.
[44] L.L. McConnell, J.A. Harman-Fetcho, J.D. Hagy 3rd, Measured concentrations of herbicides and model predictions of atrazine fate in the Patuxent River estuary, J. Environ. Qual. 33 (2004) 594–604.
[45] G. Marchetti, M. Minella, V. Maurino, C. Minero, D. Vione, Photochemical transformation of atrazine and formation of photointermediates under conditions relevant to sunlit surface waters: laboratory measures and modelling, Water Res 47 (2013) 6211–6222.
[46] D. Vione, The modelling of surface-water photoreactions made easier: introducing the concept of 'equivalent monochromatic wavelengths', Water Res 190 (2021) 116675.
[47] A. Bianco, D. Fabbri, M. Minella, M. Brigante, G. Mailhot, V. Maurino, C. Minero, D. Vione, New insights into the environmental photochemistry of 5-chloro-2-(2,4-dichlorophenoxy)phenol (triclosan): Reconsidering the importance of indirect photoreactions, Water Res 72 (2015) 271–280.